24th INTERNATIONAL CONGRESS ON SOUND AND VIBRATION
23–27 July 2017, London

CATEGORIZATION OF THE BATS SPECIES BASED ON EIGEN ANALYSIS OF BAT BIOSONAR BEAMPATTERN

Weikai He

University of Jinan, Jinan, Shandong, CHINA
Shandong University, Jinan, Shandong, CHINA
email: sps_hewk@ujn.edu.cn

Jianxiong Feng

University of Jinan, Jinan, Shandong, CHINA

Li Gao

University of Jinan, Jinan, Shandong, CHINA

The Intelligent Antenna nowadays can manipulate sound field beam pattern by modulating the phase of array antenna, while bats of different species can realize the same function by certain structure or behavior of their outer ears. Therefore, study the common features of those bats is very important for improving intelligent antenna. This research involves calculating the acoustic beampattern of 30 ears among different bat species at their specific frequencies using FEM method. Next, put all the beampatterns in one direction and compress the beampatterns using spherical wavelet, select first three eigen beam-patterns by principal component analysis. The study shows that the greater the weight of first eigen beampattern has, the more convergent the main lobe is. This means more energy concentration and helps bats to target the prey. The greater the weight of the second eigen beampatterns has, more side-lobes appears. This optimizes energy distribution and helps bats to avoid obstacles and prey. When weight of the third eigen beampatterns increased, the center of the main lobe shifts to the antarctic, which helps bats to seek prey in the vertical direction.

Keywords: Beam pattern; bats biosonar pulse; principal component analysis; finite element method; wavelet analysis.

1. Introduction

Most species of bats use their unique echo-locating system to detect the complex surrounding environment, so that they can prey and avoid the obstacles [1, 2]. In the preying process, the bats employ both active and passive sonar signal to lower the energy consumption [3]. The active sonar is emitted by bats and the passive sonar is received from the targets. In the anatomical point of view, after long time evolution, the noseleaf and pinna of the bats have formed the intricate structures, which serve as the bats sonar system.

The noseleaf has the similar function as man-made loudspeaker, while the structure of the noseleaf is much more complicated. Furthermore, different parts of the noseleaf have different acoustic function. The change of the overall shape and size of the nose can cause significant effects on the outgoing acoustic beam [8, 10]. The more detailed study revealed that, in the noseleaf, the lancet/sella and their substructure can manipulate the far-field directivity pattern [4, 5, 9]. For the signal receiving

part, the deformation of the outer ear of the greater horseshoe bats can also affect the far-field acoustic beam energy, thus facilitating the echo-localization [12].

Despite the diversity in the bats' pinna shape, they all can be used to avoid the obstacles and prey [13]. The functionality of the pinna provides inspiration for the new smart antenna design. To study the general principle of the pinna functionality, in this study, the far-field acoustic directivity patterns are calculated numerically for thirty bats, among which seven bats are FM bats and 23 bats are CF-FM bats. The geometries of the pinna model are obtained by the digital processing of the Micro-CT machine scanning. The digitally obtained model is used to calculate the far-field directivity pattern, as shown in Fig. 1. In Fig. 1, for each bats, the -3 dB contour of ten frequencies are calculated and presented. The details of the methodology and the results will be presented in the next sections.

2. Method

2.1 Finite element method

To obtain the 3D structural images of the bats ear, the high resolution X ray scanner Skyscan1072 was used (micro-computer tomography, micro-CT). The 3D numerical model was obtained by the processing of the 3D images. Then finite element method was used to calculate the bats outer ear acoustic field [5] for 30 bats. For each ear, the acoustic field for ten frequencies were calculated (Fig. 1).

2.2 Maximum inner product

The maximum inner product can turn all the sonar beams into the same direction, thus facilitating the eigen analysis of the sonar beam pattern. To unify the direction of the sonar beam, the direction of one beam should be chosen as the reference. Then rotate other sonar beams to a certain angle, which is the angle between the rotated sonar beam and the reference sonar beam using the inner product.

2.3 Wavelet analysis

Because the data sets in this study is too large (181*361=63541 points), wavelet analysis was used to compress the data. The MATLAB toolbox, Toolbox Wavelets on Meshes, was employed to perform the analysis. The pentagonal dodecahedron subdivision domain is used in this study to represent a sphere. Level 0 of contains 12 vertexes, the relationship between the level J and number of vertex N is that [14]:

$$N = 10 * 4^{J-1} + 2 \tag{1}$$

According to Eq. 0, the level 6 contains 10420 points. Performing the 6-fold subdivision to the sonar beam, we can obtain 10420 wavelet coefficients. The coefficients are rearranged in a descending order, then, only the first 1/10 coefficients are preserved and the rest are set to zero. Finally, 1024 coefficients are selected.

2.4 Principal component analysis

Principal component analysis (PCA) calculates the variance/covariance matrix of the data matrix. Then, perform eigen decomposition to the variance/covariance matrix to obtain the eigenvalues and eigenvectors. The larger the eigenvalue is, the more information the rotation can preserve. The dimension reduction is the core of the method. The eigenvectors can be calculated using the covariance matrix and eigenvalues. Then, the eigenvectors can be used to transform the data into the eigen-domain for further analysis.

In this study, all the wavelet coefficients for the sonar beam corresponding to 10 frequencies are put together and reordered descendingly. Each beam contains 1024 coefficients, thus there are 10240 coefficients for the beams of 10 frequencies. The reordered coefficients forms a vector, and each

vector contains the wavelet coefficients for one ear. In total, 30 ears are tested in this study, put 30 vectors together to form a 10240*30 matrix, which has 10240 columns and 30 rows. The physical meaning of the matrix is that 30 points exist in a 10240 dimension domain. The coordinates of the i^{th} row and j^{th} column means the projection of the i^{th} point on the j^{th} dimension. Then, the data was centered for later calculation. The variance/covariance matrix is calculated using the centered data. The eigenvalues can be obtained using the variance/covariance matrix, which is shown in Fig. 2.

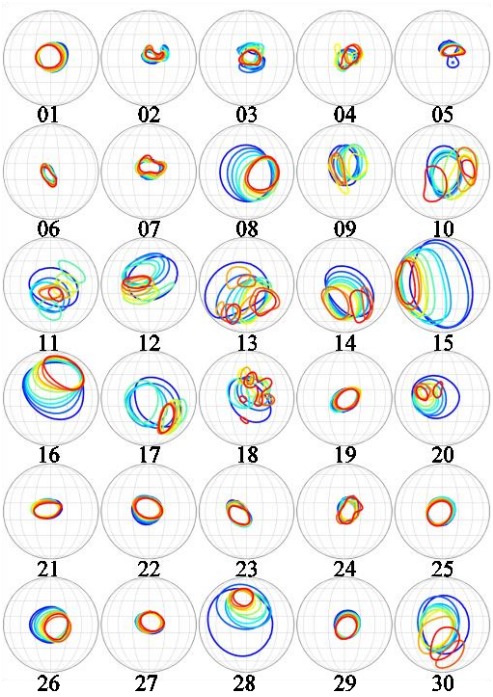

Fig. 1 The contour -3 dB contour line in the beampatterns of all 30 bats.
Different colors stands for different frequencies. Totally ten frequencies are calculated.

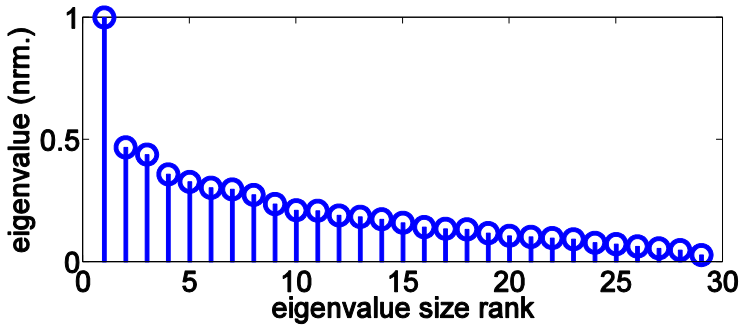

Fig. 2 Normalized eigenvalues.
The eigenvalues of the correlation matrix for all thirty bats.

2.5 Measurement of the mailobe width

To characterize the acoustical properties of the sonar beam, the convetional -3dB line is used to identify the mainlobe range. The maximum distance between the points on the enclosed -3dB line is chosen as the measure of the width of mainlobe, which is called half-power-beam-width (HPBW). The concrete procedures of measuring the mainlobe width is as follows: (1) identify the -3dB line range; (2) calculate the eigenvalues of all the angles and location; (3) the distance between the intersection points of the -3dB contour line and the directional line of the maximum width is defined as the maiblobe width.

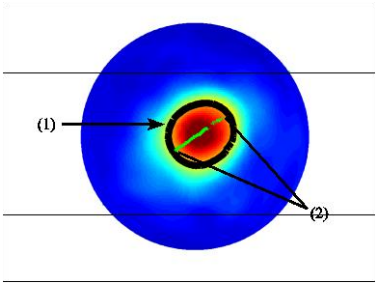

Fig. 3 Measurement of the mainlobe width.
(1) -3 dB contour line; (3) the line that represents the mainlobe width.

3. Results

The eigenvalues of 30 bats pinna were calculated using the PCA. The larger the eigenvalues is, the more important the corresponding beampattern is. Here, the beampatterns corresponding to the two largest eigenvalues are chosen for analysis. In the analysis, the first two eigenvectors multiply with different coefficients, then, they are added by the averaged acoustic fields. In the real condition, acoustic beam coefficients usually varies betweem -10 to 10. Hence, the coefficients between -10 to 10 with an interval as 2 are calculated in the simulation. Then, the two eigenvectors with the largest eigenvalues will be analyzed in details.

In the sonar beam corresponding to the first eigenvectors, as shown in Fig. 4, in the low frequencies (1-5), the area of mainlobe increases with the increase of coefficients. In the high frequencies, except for the enlargement of the mainlobe area, the sidelobes also becomes larger with the increase of the coefficient. In the sonar beam corresponding to the second eigenvectors, as shown in Fig. 5, in the low frequencies (1-5), the mainlobe width in elevation increases while the mainlobe width in azimuth does not show much change. And it is obvious that the elevation width becomes larger than the azimuth width with larger coefficients. In the high frequencies, it can be observed that the more energy is separated from the mainlobe with lower coefficients.

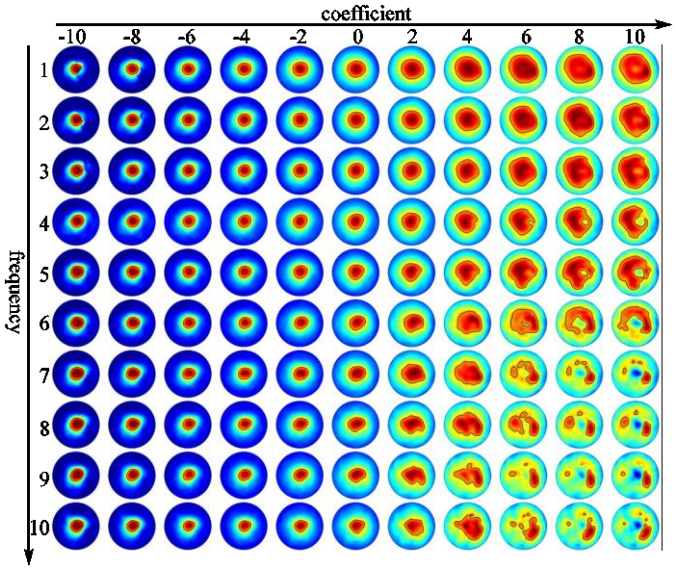

Fig. 4 The beampatterns corresponding to the first eigenvector.
Each column changes with frequency, and each row changes with coefficients.

To describe the effects of first two engenvectors on the beampatterns with different coefficients and different frequencies quantitatively, the mainlobe width corresponding to different eigenvectors are calculated, as shown in Fig. 6. In Fig.6 (a), the mainlobe width is the average of 11 different coefficients, while in Fig 6 (b), the mainlobe width is the average is 10 frequencies. As shown in Fig.

6 (a), the mainlobe beamwidth for both eigenvectors decrease with the increase of the frequencies, which match the characteristics of the general antenna system. As shown in Fig. 6 (b), the mainlobe beamwidth for the first eigenvector increases significantly with the larger coefficients, while the mainlobe beamwidth for the second eigenvector stays stable.

The first eigenvectors multiplies different coefficients can cause the change in mainlobe width in all the directions. It can be concluded that: the most essential characteristics of the bats beampattern is the mainlobe size. The smaller coeffcients can make the mainlobe smaller while the larger coefficients can make the mainlobe larger. The second eigenvectors times the coefficients, the mainlobe width change in azimuth and elevation alternatively. It can be concluded that: the second characteristics of the beampattern is the mainlobe width in azimuth and in elevation. It can be seen that when the second eigenvector multiplies small coefficients, the mainlobe width in elevation is larger than the mainlobe width in azimuth; while the mainlobe width in elevation is smaller than the mainlobe width in azimuth, if the second eigenvector multiplies small coefficients.

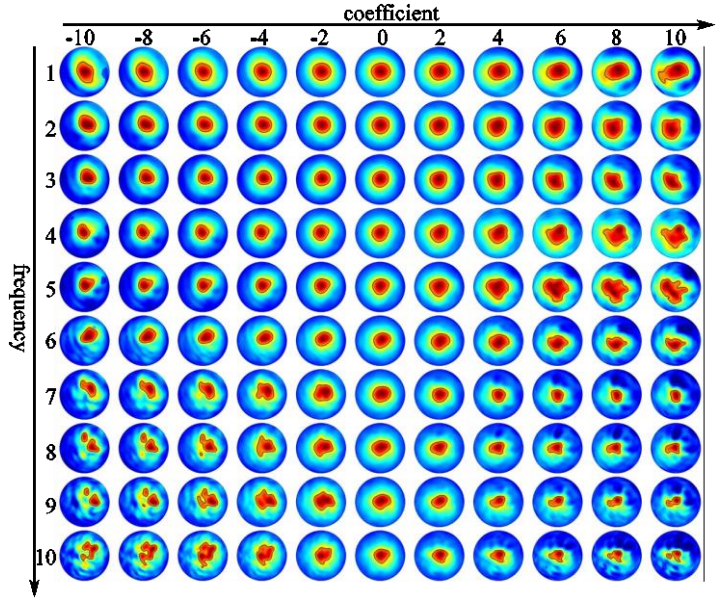

Fig. 5 The beampatterns corresponding to the second eigenvector.
Each column changes with frequency, and each row changes with coefficients.

Categorize all the 30 bats into different genus, and mark the them in the plot of distribution in both first eigen space and second eigen space, in which the bats belonging to the same genus are marked using the same label. The 30 bats used in this study can be categorized into 13 genus. In Fig. 7, only genus with more than 3 bats are plotted. As shown in Fig. 7, the bats from the same genus locate closely in the plots. In particular, the points spread over a wider range in the first eigen space than in the second eigen space. For example, all “Myotis” bats has positive values in the first eigen space while the most of the “Rhinolophus” bats have negative values in the first eigen space. Hence, it can be concluded that: the eigen characteristics of bats are related to the genus of bats, and the same genus of bats have very similar acoustic properties.

4. Conclusions

The study investigates the directivity pattern in the eigenspace for different bats， which uncovers some general characteristics of the sonar used by bats. The sonar characteristics of bats reflect the functionality of the shape of outer ear. The more detailed study reveals the relation between the shapes of the bats ear and the far-field directivity pattern. The results can be used for the antenna design.

First, the function of the antenna can be used to determine the needed beampattern. Then, the beampattern can reversely engineered to design the antenna geometry using the relationship between the geometry and the beampattern.

In addition, the eigevectors extracted using the beampatterns of the 30 bats can be used for the categorization of the bats species using the acoustic characteristics. The method can implement the traditional biological categorization approach, and improves the accuracy of the categorization.

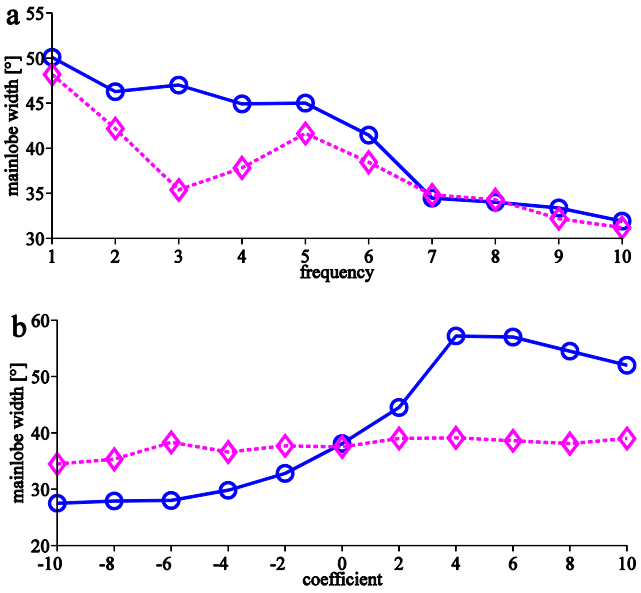

Fig. 6 The mainlobe width for first (blue) and second (red) eigenbeam.
(a) The mainlobe change with frequency; (b) the mainlobe width with different weight.

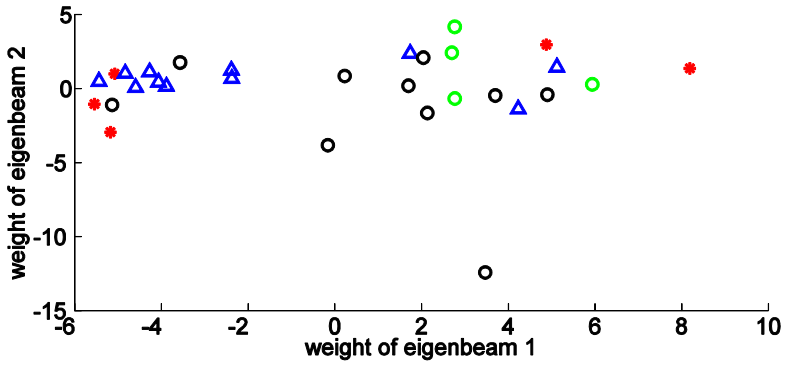

Fig. 7 The distribution of different bats in the first and second eigen space.
△: Rhinolophus; o : Myotis； *: Hipposideros； o : others。

REFERENCES

1 Müller, R. & R. Kuc: Foliage echoes: a probe into the ecological acoustics of bat echolocation. J. Acoust. Soc. Am，2000； 108(3): 836-45
2 Jone G, Teeling E C. The evolution of echolocation in bats. Trends Evol, 2006; 149-156.
3 Griffin D R. Listening in the dark. Ithaca: Cornell University Press, 1986； 57-147.
4 Zhuang. Q., Müller. R. Noseleaf furrows in a horseshoe bat act as resonance cavities shaping the biosonar beam. Phys Rev Lett, 2006; 97: 218701-4.
5 Zhuang. Q., Müller. R. Numerical study of the effect of the noseleaf on biosonar beamforming in a horseshoe bat. Phys Rev E, 2007; 76: 051902-1-11.
6 Zhang. Z., Nguyen. S. T., Müller. R. Acoustic effects accurately predict an extreme case of biological morphology. Phys Rev Lett, 2009; 103: 038701.
7 王福勋, 庄桥, 张智伟. 大耳蝠耳廓模型频扫特性的研究，声学学报，2010; Vol.35 (1): 26-30.
8 Zhang. Z., Nguyen. S. T., Müller. R. Acoustic effects accurately predict an extreme case of biological morphology. Phys Rev Lett, 2009; 103: 038701.
9 Dieter Vanderelst, Fons De Mey, Herbert Peremans, Inga Geipel, Elisabeth Kalko , Uwe Firzlaff (2010). What Noseleaves Do for FM Bats Depends on Their Degree of Sensorial Specialization. PLoSONE 5(8): e11893. doi:10.1371/journal.pone.0011893.
10 Hartley. D. J., Suthers. R. A. The sound emission pattern and the acoustical role of the noseleaf in the echolocating bat, carollia perspicillata. J Acoust Soc Am, 1987; 82: 1892-1900.
11 Rolf mueller, Hongwang Lu, and John R. Buck. Sound-diffracting flap in the ear of a bat generates spatial information. Phys. Rev, Lett., 2006, 100(10):108701.
12 Gao L, Balakrishnan S, He W, Yan Z, M¨uller R (2011) Ear deformations give bats a physical mechanism for fast adaptation of ultrasonic beampatterns. Phys Rev Lett 107: 214301.
13 Rolf Müller. Numerical analysis of biosonar beamforming mechanisms and strategies in bats. J. Acoust. Soc. Am. 2010, 128 (3): 1414–1425.
14 Peter Schröder and Wim Sweldens. Spherical wavelets: efficiently representing functions on the sphere. In Proceedings of the 22nd annual conference on Computer graphics and interactive techniques, SIGGRAPH '95, pages 161-172, New York, NY, USA, 1995. ACM.
15 S. Wold, K. Esbensen, and P. Geladi. Principal component analysis. Chemometrics and intelligent laboratory systems, 1987; 2(1):37–52.